Chapter 7:

Probing the Blue-Green Fluorescence of Marigold Petal-derived Carbon Quantum Dots for Dissecting their Interaction with Dyes

7.1 Introduction

7.1.1 The Menace caused by Food Adulteration

The malpractice of food adulteration is a very serious concern that arose many decades ago. Food trade and consumption has slowly grown with globalisation making food products more accessible and affordable. As food industry flourished, monetary profit became an important consideration for food merchants. The consumers often lack knowledge on food safety levels and unknowingly harm their own health. Often poor people introduce these toxic adulterants in their ignorance to earn profit [1]. In many countries this practice is rampant where many cases are reported regularly till date. Therefore, it has become a very important area of research for scientists to not only spread awareness on the harmful effects of these adulterants through their work but to also apply scientific principles and concepts for designing simple sensors for checking food adulteration which are affordable, give high-throughput analysis and are easily scalable for household use.

7.1.2 Common Food Adulterants in Daily Consumables

In today's day and age, food adulteration has increased manifold over the years and is at its peak. Everyday consumables are infested by unknown chemicals. This has lead to a steep rise in rates of cancer, gastrointestinal, kidney and liver dysfunctions and many more food-borne diseases [2]. In rural areas and villages, Sunset Yellow FCF, Tartrazine and Carmoisine food colours have been found to greatly exceed the

permissible limit. Non-permitted colours such as Metanil Yellow, Malachite Green, Rhodamine B, Orange II, Auramine, Quinoline Yellow, Amaranth and Sudan dyes have been identified often in various foodstuffs [3]. These non-permitted dyes also find unscrupulous use in sweets industry increasing risk in Indian population, especially in children which is a big concern [4]. Mycotoxins such as, aflatoxins, ochratoxins, fumonisins, zeralenone, patulin, and trichothecenes produced by moulds are found in food products leading to serious outbreaks of food-borne diseases [1]. Milk is the most commonly adulterated food product [5]. Adulteration of oil can even lead to gall bladder carcinoma [6]. Various kinds of synthetic colors and dyes are added in foodstuffs to produce aesthetically and psychologically attractive eatables [3,7] and to increase consumer's acceptability such as Erythrosine, Allura Red, Tartrazine, Sunset Yellow, Brilliant Blue, Indigo Carmine, all approved dyes for use by both the EFSA and the FDA [8,9]. Rhodamine B, Metanil Yellow, Orange II, Malachite Green, Auramine, Quinoline Yellow, Amaranth and Sudan dyes are not permitted and have been identified in various foodstuffs [3,7]. Green vegetables are known to be dyed by malachite green and yellow pulses often find adulteration by metanil yellow which are banned by USFDA and many developed countries [10, 11]. The most dangerous are cheap parlour icecreams containing pesticides, animal glue and a horde of harmful chemicals like pepperonil, ethylacetate, butraldehyde, emil acetate, nitrate and washing powder. Residues of endosulfan, cypermethrin, dimethoate, monocrotophos and mancozeb were detected in tomato, eggplant, okra, cabbage and cauliflower collected from the market [1]. In order to shed light and stop this malpractice, it has become extremely important to stay updated with food research and design simple sensors for the detection of these unwanted chemicals for households. Food-borne diseases are a common occurrence worldwide. Still, even

today, consumers have little knowledge about adulteration in their daily food since it is difficult to assess the ill-effects of chronic exposure of chemicals in humans. This project is aimed at highlighting and mitigation of this problem by ensuring food safety measures through proper study which will have an impact on prevention of health hazards and strengthening of regulatory system. This work will further help in spreading awareness on these issues and finding sustainable simple and affordable solutions to detect adulterants.

7.1.3 Introduction to Carbon Quantum Dots as Detection Tools against Food Adulteration

Carbon quantum dots (CQDs) have made a considerable space in the scientific arena by being a valuable tool in various biomedical and biosensing applications because of their brilliant fluorescence, biocompatibility, ease of synthesis and flexibility in choice of the carbon starting material [12,13]. They are strong competitors for their semiconductor counterparts which have a wide fluorescence range, high quantum yield and huge potential in LED and optoelectronic applications [14]. Nevertheless, they are toxic and have multiple complicated steps as compared to carbon quantum dots. The organic structure of CQDs strongly resonates in most biota making its use in living systems more feasible. Their bright fluorescence offers much potential for sensing various analytes [15]. In this work, their capability to sense common food adulterants has been explored by devising a facile spectroscopic detector using CQDs.

CQDs have been synthesized using a wide array of natural sources like hair, fruits, feathers, grass, urine and meat [16-21]. Many methods of CQD synthesis are successfully used like arc discharge, laser ablation, acid reflux, microwave-assisted,

sonication and hydrothermal method [22]. Out of these methods, hydrothermal method has proven to be one of the simplest ways of producing CQDs in a one-pot synthesis step. Because of its simplicity and popularity in the field of CQD synthesis, in this work this method has been harnessed to understand the effect of different physical paramaters on the quantum yield of the synthesized CQDs. These include temperature, solvent, addition of ions and variation in the carbon precursor used.

7.1.4 The Choice of Carbon Precursor for CQD Synthesis: *Tagetes* corolla

The choice of the carbon precursor for this objective is the corolla of marigold (*Tagetes erecta/pucida*). Marigold is a common plant native to many parts of the world used in indigenous traditional ceremonies. The flower of this plant comes in multiple shades. Three colours are commonly native indigenously and were chosen as the starting material for the reaction- orange, yellow, brown. Through the same hydrothermal synthesis route, using the same plant for producing CQDs, the process was subjected to physical and minute compositional differences. This set of experiment would greatly help in understanding the effect of changing each of these conditions on the fluorescence properties of the final CQDs. Systematic chart would enable relating each condition with a fair prediction of the probable fluorescence of CQDs when a new natural carbon source is being utilized.

7.1.5 Application of CQDs in the Detection of Food Adulterant Dyes

The highly fluorescent CQDs thus generated can be incorporated into a food adulterant detection device for sensitive sensing. The combination of few CQDs could ensure more selective and accurate detection due to the difference in the dynamic complex of the adulterant and the CQD surface. The interactions can cause emission peak shift, quenching, FRET or even no significant change from the previous

photoluminescence. These signals collectively differ for each dye and as such can be used for the detection of multiple dyes through a single device.

7.2 Results and Discussions

This chapter includes a report on utilizing the blue-green fluorescence of carbon quantum dots for specific detection of adulterant dyes; in this case, malachite green has been used as the model dye. CQDs using marigold petals as the carbon precursor have been synthesized via the hydrothermal method. These CQDs have been subjected to different physicochemical conditions including solvent, temperature, acidic and basic environments. Moreover, three different species of the same plant, *Tagetes*, were chosen to observe the difference based on innate and minute alterations in structural composition. Four CQDs from these combinations with maximum quantum yield were chosen for designing a dye-specific sensor for application in food adulterant detection. In this study, malachite green has been used as a model dye.

7.2.1 The Synthesis of CQDs using the Corolla of *Tagetes* cultivars

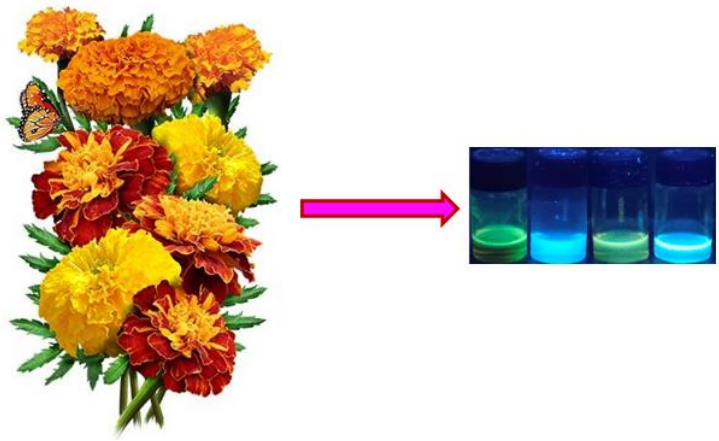

Figure 7.1: Synthesis of Blue-Green CQDs using marigold (*Tagetes*) cultivars

Three cultivars of marigold (*Tagetes erecta/pucida*) were chosen as the carbon precursor for differently conditioned hydrothermal reactions to synthesize carbon

quantum dots. It was hypothesized that most molecular components would be similar since they were derived from the same plant, marigold. It was interesting to note what differences in the final extracted CQDs would result from changes in pigment and minute compositional variations. Towards this effect, three coloured corrollae, (orange, yellow, brown) were picked as the starting material. Individually, each of these coloured petal-set was immersed in six different solvents for extraction. Moreover, 1 mN NaOH or 1 mN HCl was combined into each solvent to introduce a set acidity/basicity into the extract. As observed through Figure 1, all permutations yield different fluorescence colour and brightness, but mostly falling within the blue-green wavelength range. The brightest CQDs were composed in ethanol and PEG solvents. The dullest CQDs with limited fluorescence were observed in acetone and DMSO. This clearly shows the role of solvents in directing the multistep reaction and playing the surface effect by interacting with the highly electron active functional-group rich surface of the formed CQDs.

A notable observation was the diminished photoluminescence in the case of 1 mM HCl added solutions for all solutions subjected to 120°C hydrothermal temperature. However, at the same temperature, just by adding 1 mM NaoH drastically altered the final CQD fluorescence. That is not to say that protonation of the solution did not yield brighter fluorescence in any case as seen for 3W180A and 1E180A written in short. Here, the first digit stands for the corolla set, the capital letter for the solvent initial followed by the hydrothermal temperature and addition of acid (A) or base (B). Majorly, the solutions with the base added displayed brighter fluorescence. This experiment also allows one to assess the role of the starting precursor material for the CQDs. The solutions drawn from the yellow-petalled marigold yielded CQDs with brighter photoluminescence as compared to orange and

least fluorescent brown petals. Water, PEG and ethanol as solvents yield fluorescent CQDs constantly over the multiple hydrothermal conditions as opposed to acetone and DMSO. Isopropanol offers decent fluorescence to CQDs more red-shifted than most samples (120B). Naturally, CQDs are more fluorescent at reaction temperatures set at 180°C for the hydrothermal reaction. From all these reaction combinations, four fluorescent samples were selected based on maximum quantum yield for further examination. These were 2D120B, 3W180A, 1E120B and 1E180A.

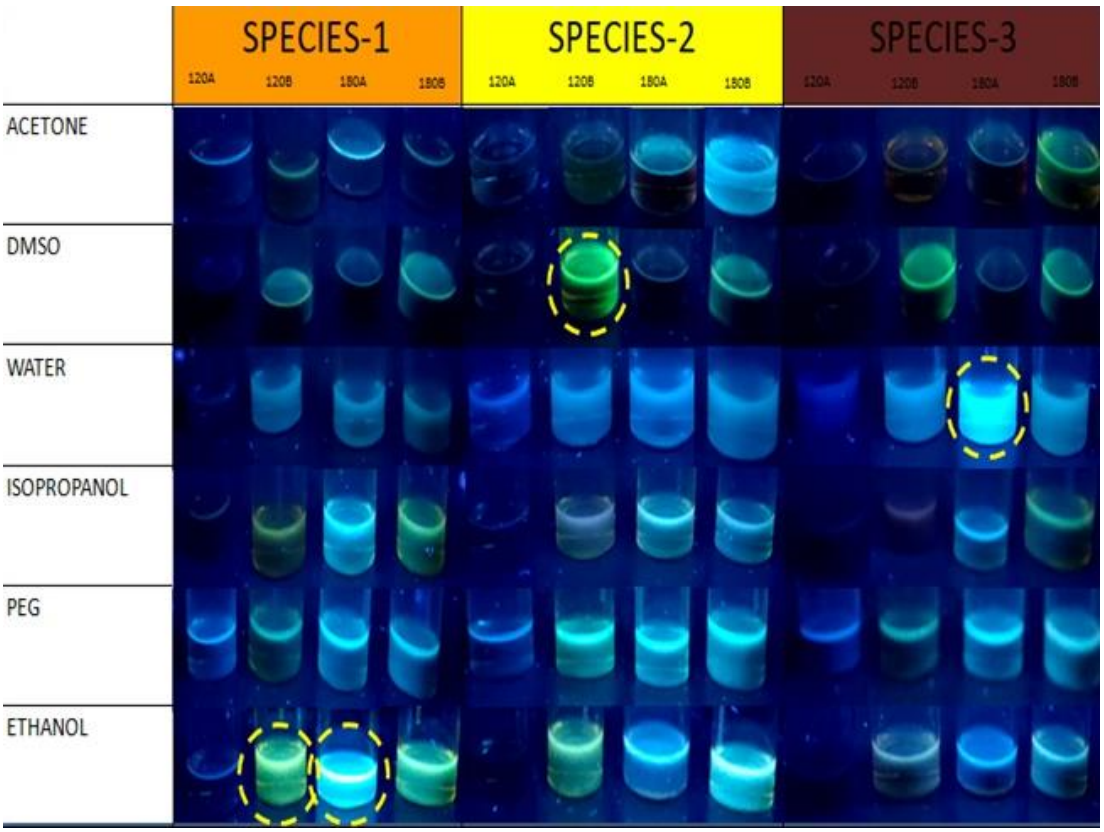

Figure 7.2: CQDs Synthesized by employing variants in the hydrothermal reaction: Colour of marigold flower petal, solvent, hydrothermal temperature, addition of NaoH/HCl

7.2.2 Selection and Characterisation of Chosen CQDs with Highest Quantum Yield

The four CQDs selected were green (solvent: DMSO) and blue (solvent: water, ethanol). All the samples showed unique emission owing to the specific reaction condition set for each of them (Figure 7.3A). The CQDs synthesized using water as the solvent (3W180A) was used as reference to check the effect of hydrothermal temperature further on the fluorescence of CQDs. It was observed that fluorescence only slightly appeared in samples subjected to a hydrothermal temperature of 100°C. Emission increased slightly around 150°C and was best at 200°C (Figure 7.3B). This shows that as the reaction temperature increases, the molecular structures in the system gradually get dehydrated to form carbonaceous centres of luminescence. At lower temperatures, the fluorescence mostly originates from the molecular luminescent centers while at higher temperatures the carbon dots are more defined cores with a functionally active surface acting as the centers from where fluorescence originates. The absorbance spectra have been recorded for the four CQD samples (Figure 7.4C-F). It is observed that most CQDs absorb n the UV-blue region as is expected by their emission and is common to most CQDs synthesized through hydrothermal method using natural precursors. The slight shoulders may indicate the π-π^* and n-π^* electronic transition of C=C/C=N and C=O bonds. The minor changes may result from the differences in reaction conditions and the solvent effect. The zeta potential of the four CQDs was also calculated to understand the charge distribution on the surface of the CQDs. It was observed that all CQDs possessed an electronegative zeta potential ranging from -20 to -10 mV. This result shows that these CQDs are very stable in solution and would not aggregate easily to form larger clumps that could depreciate the optical properties of CQDs over time. These samples were found to be stable for the three month duration they were observed. This result shows

that these CQDs can be used for applications that require fluorescence stability of CQDs over a long duration.

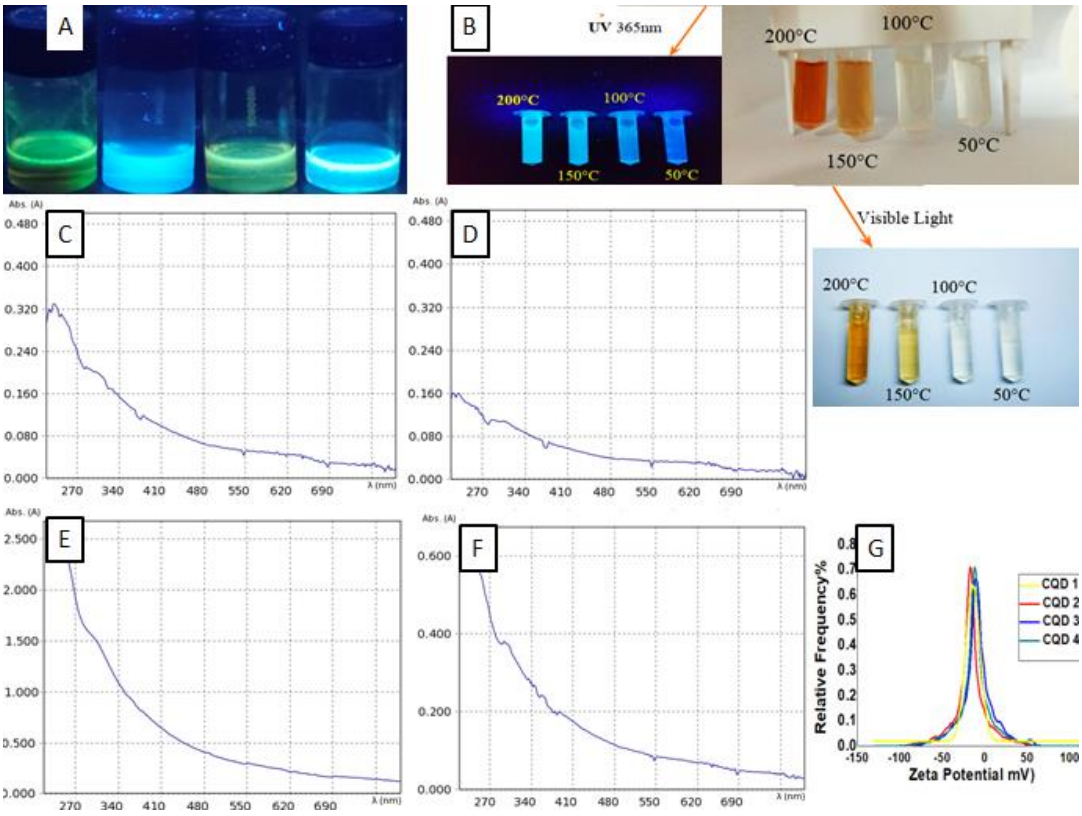

Figure 7.3: Four CQD samples selected with highest quantum yield (A) CQD samples: 2D120B, 3W180A, 1E120B, 1E180A (B) Hydrothermal temperature of 3W180A extract from 50C-200C (C-F) UV-Vis Absorbance spectra of CQD samples (G) Zeta potential of CQDs

The quantum yields of the four CQD samples were calculated to be within a range of 10-35%. These values are good for exploitation in sensing applications. They are higher than most average quantum yields of CQDs derived from natural sources synthesized by the hydrothermal method. They were estimated using quinine sulphate as reference in 0.1 M H_2SO_4. Higher quantum yields have been proposed to originate from the hydroxyl, amide and other groups that help in suppressing the non-radiative transfer of energy which eventually leads to an increased photoluminescence.

7.2.3 Photoluminescence Spectra of the Four Selected CQDs

The PL spectra of the four CQD samples were computed to understand their fluorescence behaviour (Figure 7.4). The origin of photoluminescence in carbon quantum dots has been a matter of debate for a long time. Many hypotheses have been offered like the radiative recombination of electron-hole pair. It is also thought that the fluorescence mechanism originates from the core of CQDs where the carbon-carbon sp^2 clusters form a condensed fluorophore due to quantum confinement or the surface states dominate to form the electron-active emissive traps facilitated by the oxygen and nitrogen containing surface functional groups, defects and zig zag edges. The solvent plays an important role in influencing the surface state of the CQD. The difference in size distribution may make CQDs appear as wavelength-independently fluorescent. In this case, 2D120B showed a good PL distribution in the blue-green region extending till 700 nm. The emission maxima falls around 485 nm at an excitation wavelength of 320 nm (Figure 7.4A) responsible for its distinct green hue. For 1E180A, the emission maxima lay close to 430 nm at an excitation wavelength of 340 nm (Figure 7.4B). For 1E120B, the maximum emission was close to 440 nm at an excitation wavelength of 340 nm (Figure 7.4C). 3W180A demonstrated a clear fluorescence peak centering at 459 nm at multiple excitation wavelengths (Figure 7.4D). These spectra demonstrate the broad spread of the PL emission from these CQDs making them robust candidates for using them in various applications.

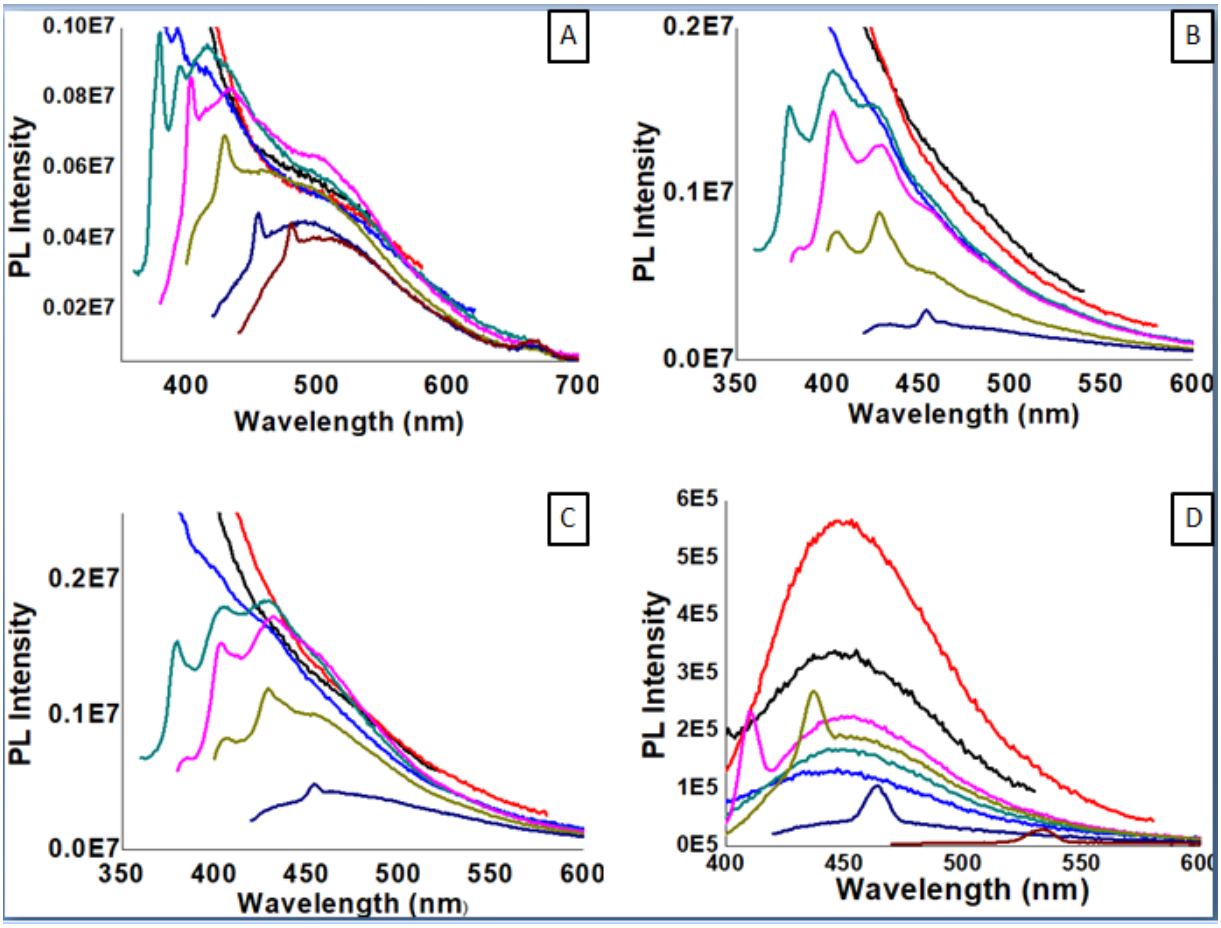

Figure 7.4: PL spectra of the four CQD samples. Fluorescence spectra of (A) 2D120B at various excitation wavelengths starting from 280 nm (B) 1E180A at various excitation wavelengths starting from 280 nm (C) 1E120B at various excitation wavelengths starting from 280 nm (D) 3W180A at various excitation wavelengths starting from 280 nm

7.2.4 Elucidation of the Morphological Characteristics of CQDs

Further these CQDs were characterised for their morphological and structural information through TEM analysis. The CQDs were found to be fairly uniformly distributed with a narrow size distribution range (Figure 7.5A-D). The TEM images of 2D120B, 3W180A, 1E120B and 1E180A were recorded at 100 nm resolution. The ethanol-based CQDs were smaller in size as compared to the other CQDs. DMSO-dispersed CQDs were bigger and closer while water-based CQDs were more distantly spread. All CQDs showed typical quasispherical morphology showing the completion

of the multistep reactions responsible for the formation of CQDs. The X-ray diffraction plots confirmed the amorphous nature of the CQDs indicated by the absence of sharp peaks and a broad peak centering around 24° 2θ values (Figure 7.5E). This is in agreemeny with the (002) plane of graphitic materials with a high disorder in the lattice where the interlayer lattice spacing is close to 3.33 Å showing poor crystallization.

FTIR was performed to shed some light on the structural composition of CQDs by revealing the surface functional groups (Figure 7.5F). These functional groups mainly comprise of oxygen and minute quantities of nitrogen conjugated to carbon. The first broad peak around 3400 cm^{-1} indicates the rich presence of hydroxyl groups and partial existence of secondary amines and amides. Peaks near 2900-2800 cm^{-1} signify the presence of alkyl side groups. The peak at 1726 cm^{-1} denotes the presence of C=O of aldehyde/ketone/carboxylic groups. The next peaks around 1620 cm^{-1} represent alkene stretch/ amine bends. The two peaks at 1413 cm^{-1} and 1453 cm^{-1} shows the presence of alkyl bending. Lastly, the peaks at 1028 cm^{-1} and 1080 cm^{-1} indicate the carbonyl vibration stretch. These groups confer polarity, hydrophilicity and biocompatibility to the CQD samples. The shifts are dictated by many factors, the compositional difference, solvent, temperature and addition of positive charges into the system.

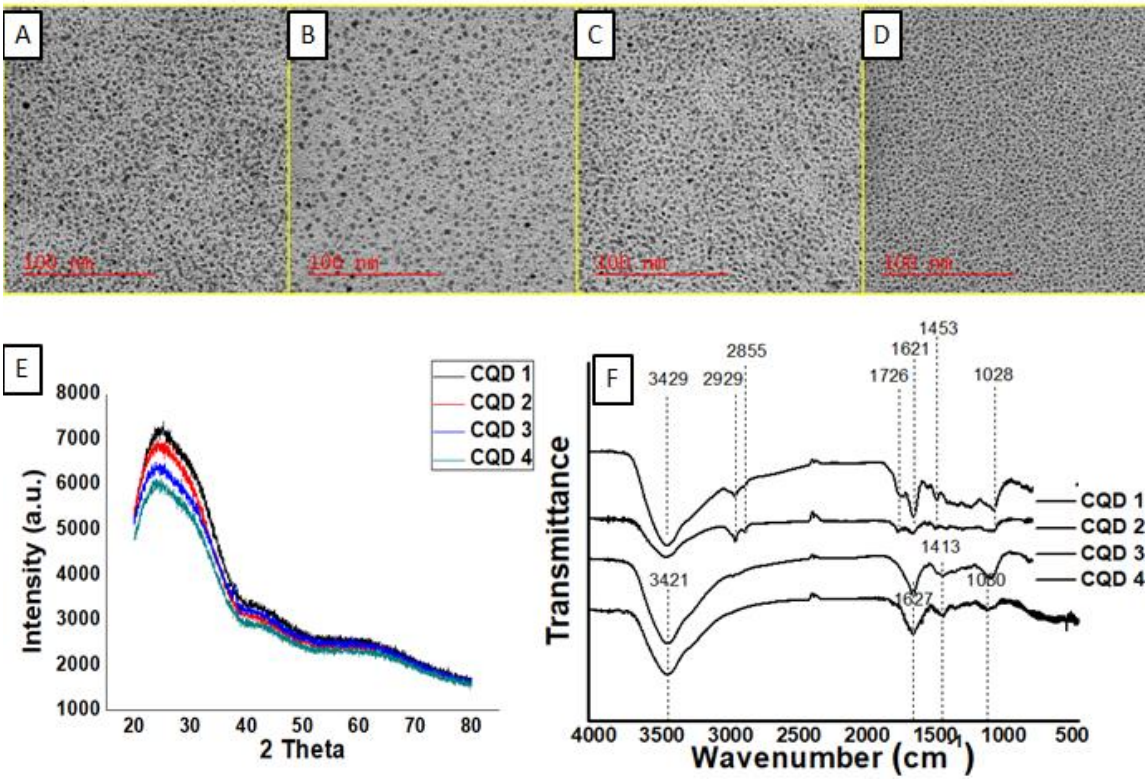

Figure 7.5: Characterisation of CQDs. (A-D) TEM analysis of CQDs- 2D120B, 3W180A, 1E120B, 1E180A (E) XRD profile of the four CQD samples-2D120B (1), 3W180A (2), 1E120B (3), 1E180A (4) (F) FTIR spectra of the four CQD samples 2D120B (1), 3W180A (2), 1E120B (3), 1E180A (4)

7.2.5 Use of the Four Selected CQD Samples for Developing an Adulterant Detection Device

The characterisation of all the four CQD samples further encouraged the utilization of these materials for the detection of adulterant dyes in daily food consumables. Although many sophisticated methods have been proposed for such detection, in practical everyday use, they prove to be ineffectual. CQDs have extensively been explored for their potential use in biosensing and chemical sensing. Here, these four CQDs are developed into a multi-detection device for detection of adulterants in everyday food consumables. The idea behind this objective is that the interaction between any adulterant with each of the selected CQD samples would be

specifically different. This difference can easily be monitored to design a simple detection system which is capable of detecting multiple adulterant dyes.

Towards this direction, malachite green has been chosen as a model dye. It is a triarylmethane emerald-coloured dye having a typical absorbance spectrum (Figure 7.6A). It has 3 peaks at 320 nm, 425 nm and 615 nm. The absorbance/emission profile of CQDs shows a significant overlap with the absorbance spectrum of malachite green hinting at possible dynamic interactions that might shift the PL peaks differently for each of the CQD sample (Figure 7.6B).

7.2.6 The Interaction of Malachite Green with G-Quadruplex

Malachite green has been reported to cause significant damage to DNA, the universal genetic material of most eukaryotic organisms. This leads to mutagenesis, damage to vital organs and cancer. DNA often forms secondary structures having a functional role in the cyto-niche. Of the many such self-assembled structures, G-quadruplex is a three-dimensional structure formed by four strands of guanine-rich DNA sequences. This particular sequence is richly distributed in the telomeric region of a chromosome responsible for vital aging related processes. DNA sequence that self-assembles in a suitable buffer, was designed as follows- 5'-TGGCCAAAAAAGGGCTTATCAAGGGTTGCAGGGACCTAA-3'. Malachite green was slowly added in 20 µl increments to generate very unusual fluorescence spectra of the dye itself (Figure 7.6C). This fluorescence arises from malachite green itself which is neglegible in solution but on rigidifying the lattice plane conformation by restricting motion in any dimension, red emission is observed. This happens when the tri-ringed structure of the dye interacts with the cross-sectional surface of the DNA

G-quadruplex or may even embed within the structure. This interaction prevents the rotational freedom of the rings and leads to radiative electron transitions.

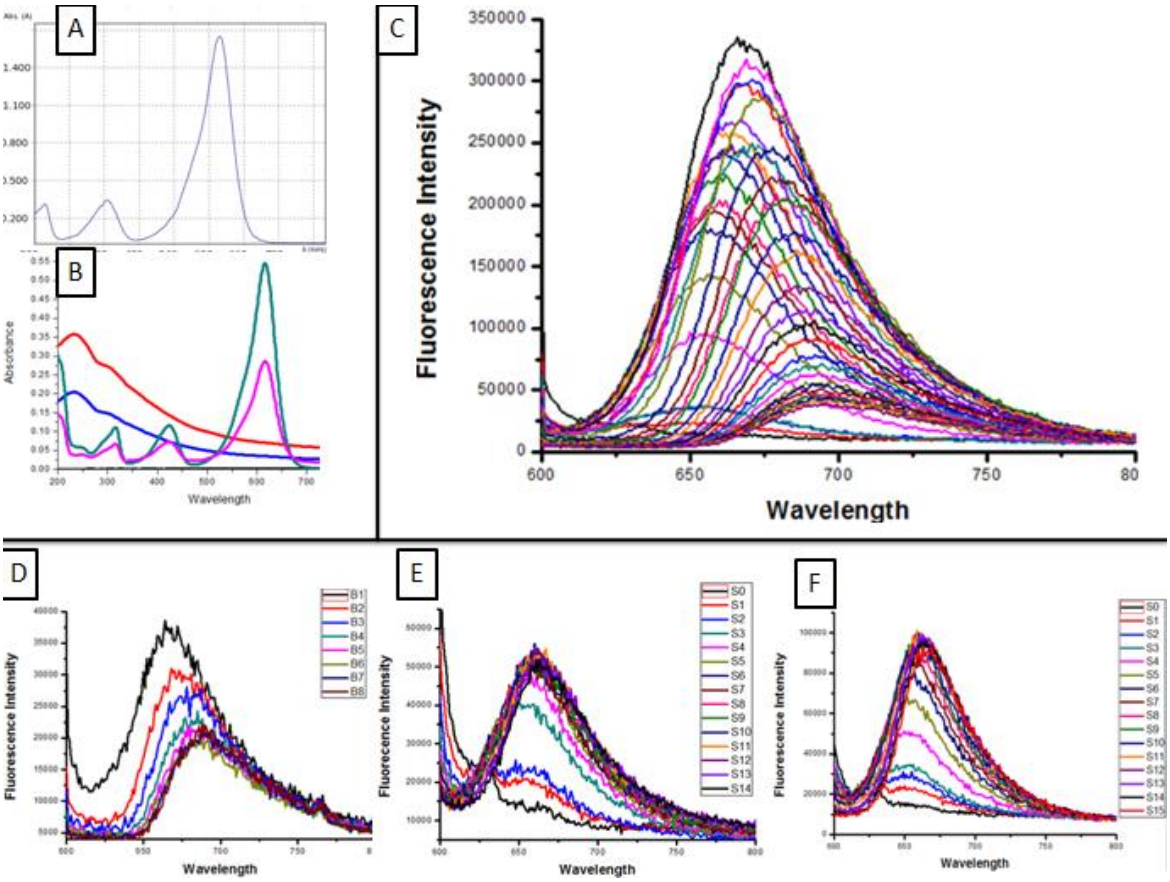

Figure 7.6: Optical Assessment of MG with CQDs and DNA secondary structure G quadruplex (A) Absorbance profile of malachite green (B) Absorbance overlap between MG and WCQD (C) Fluorescence spectra of malachite green in the presence of a designed G-quadruplex sequence 1 (D) Fluorescence spectra of malachite green in the presence of a designed G-quadruplex sequence 2 (E) Fluorescence spectra of malachite green in the presence of a designed G-quadruplex sequence 3 (F) Fluorescence spectra of malachite green in the presence of a designed G-quadruplex sequence 4

The same process of incremental addition of MG was done with similar DNA sequences capable of forming independent G-quadruplexes (Figure 7.6D-F). Although, MG showed emission in the 650-700 nm range, after a point additional MG concentration did not significantly change the fluorescence peak where emission got saturated. This shows how minute structural variations in DNA can have an effect on

the emission of these fluorophores which can effectively be used for many biosensing applications. In turn, the high affinity of MG for DNA, probably through electrostatic and π–π interactions may significantly damage the functional DNA structure leading to mutagenesis and cancer.

7.2.7 Prototype Device Design for Detecting Food Adulteration

Adulteration of most food items that are consumed daily is a malpractice that needs to be noticed by making consumers aware of the possible food product adulteration. Unethically, green vegetables are adulterated by dipping them in dye solutions for example, malachite green, which has been taken here as a model dye (Figure 7.7A&7.7B).

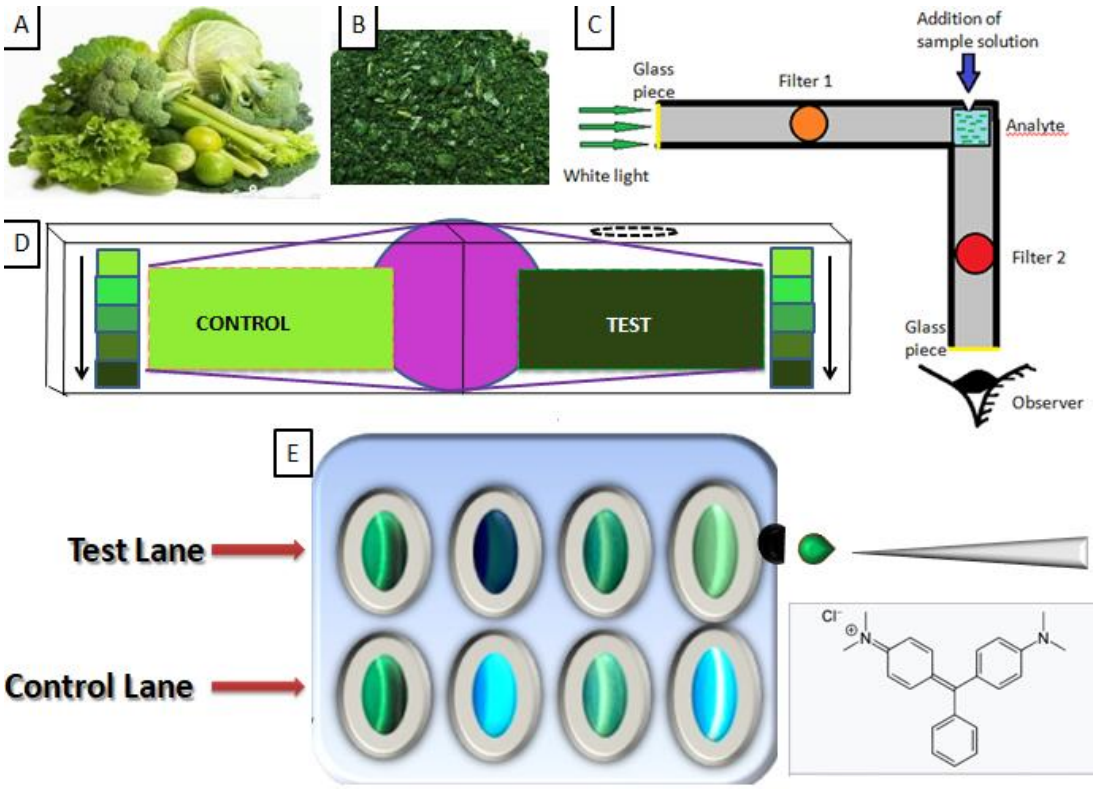

Figure 7.7: Detection of Food Adulterant Dyes Using a Single Facile Device (A) Regular Vegetables Exposed to dyes like MG (B) Malachite green dye, a common adulterant of green vegetables (C) Schematic to Utilise the Unusual Red Fluorescence of Malachite Green for its Detection in Food (D) Prototype Design of a Colour-coded Detection Device utilising the Optical Difference in Dye Quenching versus Normal CQDs (E) Built-in device with 4 CQDs utilising different interactions with the same dye to generate a unique signal for each individual dye

The presence of a dye can be detected through many sensing designs that can easily be detected spectroscopically. Carbon dots are supreme tools because of their excellent optical properties for being employed as a sensor. MG does not fluoresce in solution but on introducing constraints on its movement about the ring axis gives a beautiful red fluorescence to the dye. This mechanism can be used for the detection of this dye by incidenting the excitation wavelength on the adulterant solution and check for fluorescence through a red filter (Figure 7.7C). This kind of detection strategy can be taken a bit further by using carbon quantum dots for simple quenching of the CQD fluorescence by the sensitive interaction of MG with CQD to provide an optically distinguishable measure of MG concentration through a calorimetric sensor (Figure

7.7D). The level of quenching would be directly proportional to the amount of MG in solution and can be compared with a colour-coded label to estimate MG concentration.

Here, a multi-signal CQD sensor probe has been fabricated for a very specific detection of a dye, in this case MG (Figure 7.7E). Four CQD chambers have been designed for filling with the stable selected CQD solutions. Using the difference in the dynamic interactions between the dye and the respective CQD, different signal changes are expected if MG is exposed to the solution through the adulterated sample. With CQD 1, MG does not cause any drastic change in the signal because of non-overlap between the absorbance and emission of the dye and the CQDs. The fluorescence of the second CQD gets quenched immediately on exposure to any trace of MG in the adulterant solution because the dynamic interaction between the two causes the absorption of the fluorescenct emission of the CQDs by the MG molecules at 425 nm. The third CQD solution gets partially quenched giving a weak dip in the fluorescent signal because of the partial overlap of the two spectra for absorbance and fluorescence. Lastly, the CQD emission coinciding with the absorbance peak of MG at 425 nm converts to a FRET signal in proximity and the red-shifted emission now falls in the green region. All these changes clearly indicate the presence of a dye in certain or in future can further be converted into an electrical signal for a positive presence or absence of an analyte. Similarly, many dyes can be used for being detected by the same ultra-sensitive four-CQD design by a different cumulative signal. The signal generated by the presence of an adulterant dye can be matched with a reference signal database and within one device multiple adulterants can be detected. Few examples include methylene blue, trypan blue in edibles, metanil yellow, naphthol yellow in pulses, rhodamine B, orange G and auramine in sweets and confectionary. All these dyes contain ringed structures that interact with CQDs through dynamic collisions and

may get adsorbed either by the utilization of surface functional groups or through π-π interactions. This as a consequence affects each of the photoluminescence mechanisms of the four CQD samples differently generating a unique pattern. This pattern can be deciphered for the detection of these dyes and also to know their concentration.

7.3 Conclusions

In summary, this work involved the use of different CQDs synthesized from the same carbon precursor source, marigold petals, via the facile green hydrothermal method. A combination of different physical parameters was employed to see the difference in the photoluminescence properties of CQDs like different cultivars, temperature (120°C and 200°C), solvent (acetone, DMSO, water, isopropanol, PEG, ethanol) and addition of hydrogen/hydroxyl ions. The trend for for fluorescence of CQDs was recorded to show that higher temperature, petals with lighter hue and addition of hydroxyl ions was directly proportional to higher quantum yield. The impact of solvent effect was also seen. Out of all the permutations, four CQD samples were selected with highest quantum yield as candidates for further assessment. Further, they were used for selective detection of adulterants; here malachite green was taken as a model dye. Malachite green has elusive fluorescence properties which get enhanced on constraining movement about its rings and gives unusual PL spectra with DNA G-quadruplex secondary structure. The interaction of the dye with CQDs produces optical changes in fluorescence which can easily be converted into electrical signals for recording. The same device can be utilized for multi-detection of many dyes in general food consumables. Such strategies could prove to be very convenient for daily customer use.

7.4 References

[1] R. T. Gahukar Food adulteration and contamination in India: occurrence, implication and safety measures. International Journal of Basic and Applied Sciences, 3 (2014) pp. 47-54

[2] R. K. Sharma, M. Agrawal, F. Marshall. Heavy Metal Contamination in Vegetables Grown in Wastewater Irrigated Areas of Varanasi, India. Bull. Environ. Contam. Toxicol., 77 (2006) pp. 312–318

[3] M. Tripathi, S. K. Khanna, M. Das. Surveillance on use of synthetic colours in eatables vis a vis Prevention of Food Adulteration Act of India. Food Control, 18 (2007) pp. 211–219

[4] S. Dixit, S. K. Khanna, M. Das. All India Survey for Analyses of Colors in Sweets and Savories: Exposure Risk in Indian Population. Journal of Food Science, 78 (2013) pp. 642–647

[5] T. Azad and S. Ahmed. Common milk adulteration and their detection techniques. International Journal of Food Contamination, 3 (2016) pp 1-9

[6] R. Dixit, P. Srivastava, S. Basu, P. Srivastava, P. K. Mishra, V. K. Shukla. Association of Mustard Oil as Cooking Media with Carcinoma of the Gallbladder. J Gastrointest Canc, 44 (2013) pp. 177–181

[7] Sangita Bansal, Apoorva Singh, Manisha Mangal, Anupam K. Mangal amd Sanjiv Kumar. Food adulteration: Sources, health risks, and detection methods. Critical Reviews in Food Science and Nutrition, 57 (2017), pp. 1174-1189

[8] Sudershan, R. V., Pratima Rao, Kalpagam Polasa. Food safety research in India: a review. Asian Journal of Food and Agro-Industry, 2 (2009) pp.412-433

[9] Shubham Yadav. Edible oil adulterations: Current issues, detection techniques, and health hazards. International Journal of Chemical Studies, 6, (2018) pp. 1393-1397

[10] D. Shukla, F. P. Pandey, P. Kumari, N. Basu, M. K. Tiwari, J. Lahiri, R. N. Kharwar, A. S. Parmar. Label-Free Fluorometric Detection of Adulterant Malachite

Green Using Carbon Dots Derived from the Medicinal Plant Source Ocimum tenuiflorum, Chemistry Select, 4 (2019), pp. 4839 –4847

[11] S. Dhakal, K. Chao, W. Schmidt, J. Qin, M. Kim and D. Chan. Evaluation of Turmeric Powder Adulterated with Metanil Yellow Using FT-Raman and FT-IR Spectroscopy. Foods, 5 (2016)

[12] Z. Peng, X. Han, S. Li, A. O. Al-Youbi, A.S. Bashammakh, M. S. El-Shahawi, R. M. Leblanc. Carbon dots: Biomacromolecule interaction, bioimaging and nanomedicine, Coord. Chem. Rev. 343 (2017) 256–277

[13] J. Wang, J. Qiu. A review of carbon dots in biological applications, J. Mater. Sci. 51, pp. (2016) 4728–4738

[14] Y. Wang and A. Hu. Carbon quantum dots: synthesis, properties and applications. J. Mater. Chem. C, 2 (2014) pp. 6921-6939

[15] S. Tao, S. Zhu, T. Feng, C. Xia, Y. Song, B. Yang. The polymeric characteristics and photoluminescence mechanism in polymer carbon dots: A review, Mat.Today Chem. 6 (2017) pp. 13-25

[16] S. Liu, C. Wang, C. Li, J. Wang, L. Maoa and S. Chen. Hair-derived carbon dots toward versatile multidimensional fluorescent materials. J. Mater. Chem. C, 2 (2014) 6477-6483

[17] V. N. Mehtaa, S. Jha, H. Basuc, R. K. Singhal, S. K. Kailasa. Sens. Actuators B 213 (2015) pp. 434–443

[18] R. Liu, J. Zhang, M. Gao, Z. Li, J. Chen, D. Wub and P. Liu. A facile microwave-hydrothermal approach towards highly photoluminescent carbon dots from goose feathers, RSC Adv., 5 (2015) 4428-4433

[19] S. Liu, J. Tian, L. Wang, Y. Zhang, X. Qin, Y. Luo, A. M. Asiri, A. O. Al- Youbi, X. Sun, Adv. Mater. 24 (2012) 2037

[20] J. B. Essner, C. H. Laber, S. Ravula, L. Polo-Paradab and G.A. Baker. Green Chem., 18 (2016) 243-250

[21] J. Wang, S. Sahu, S. K. Sonkar, K. N. Tackett II, K. W. Sun, Y. Liu, H. Maimaiti, P. Anilkumar and Y. Sun. Versatility with carbon dots – from overcooked BBQ to brightly fluorescent agents and photocatalysts RSC Advances, 3 (2013) 15604-15607

[22] P. Namdaria, B. Negahdarib and Ali Eatemadi. Synthesis, properties and biomedical applications of carbon-based quantum dots: An updated review Biomed & Pharmacotherapy 87 (2017) pp. 209–222